SESSION 8.

LUMINOUS STELLAR CONTENT OF THE GALAXY-INTEGRATED PROPERTIES-II.

Chairman : M.FEAST.

1. P.MEZGER: Luminous Stellar Content of the Galaxy: Inferences from Radio and Infrared Data.

https://doi.org/10.1017/S0074180900149435 Published online by Cambridge University Press

LUMINOUS STELLAR CONTENT OF THE GALAXY: INFERENCES FROM RADIO AND INFRARED DATA

P. G. Mezger
Max-Planck-Institut für Radioastronomie
Auf dem Hügel 69
5300 Bonn 1, F.R.G.

ABSTRACT. Lyman continuum (Lyc) photon production rates can be estimated from radio free-free emission and used to estimate the star formation rate (SFR) of O stars. If this SFR is linked to the total SFR through a constant IMF ($m \gtrsim 0.1\ m_\odot$) one derives for our Galaxy a present-day SFR of $\sim 10\ m_\odot\ yr^{-1}$, which is close to the average SFR over the age of the galactic disk. This is difficult to reconcile with a formation law of the form $SFR\ \Psi \propto M_{gas}^{k}$ with $k>0$ which yields SFRs which decrease with time. Even more severe is the fact that the mass distribution of the galactic disk cannot be reproduced by the present-day SFR with a constant IMF. Bimodal star formation, however, reduces the rate at which matter is permanently locked up in low mass and dead stars by nearly a factor of three, and gets reasonable agreement between the present-day distribution of stellar mass and lock-up rate. Bimodal star formation means that stars with $m > 0.1\ m_\odot$ form in the interarm region while in spiral arms induced star formation produces only stars with $m > m_c \sim 2\text{-}3\ m_\odot$.

Our Galaxy emits about one third of its stellar luminosity as IR emission from dust. Warm (30-40 K) dust is heated by OB stars. Most of the hot (250-500 K) dust is heated by M giants with heavy mass loss, whose progenitors appear to be stars with $\sim 2\text{-}8\ m_\odot$, and which have a similar radial distribution as OB stars. From an estimate of their present-day luminosity we arrive at the conclusion that the SFR of stars with $m \gtrsim m_c$ was about constant over the past 10^8 yr.

Observations of radio recombination of H and He show that the Lyc photon radiation field gets softer with decreasing galactocentric distance. This effect is linked to an increase of the metal abundance towards the galactic center. This can be attributed to the combined effect of UV line blanketing, increase of stellar radius and decrease of the upper mass limit of the IMF.

Stellar parameters and observable radio and infrared characteristics of HII regions.

Practically all radiation of a massive, hot and luminous star surrounded by gas and dust of sufficiently high column density is absorbed and re-

C. W. H. De Loore et al. (eds.), Luminous Stars and Associations in Galaxies, 479–495.

emitted as radio and infrared (IR) radiation. The number of Lyman continuum (Lyc) photons, N'_{Lyc}, absorbed per second by the gas is related to the free-free flux density S_ν (in Jy) at a frequency ν (in GHz) high enough so that opacity effects are negligible, by

$$N'_{Lyc} = a(\nu,T_e)(1+y^+)^{-1}\ 4.76\ 10^{48}\ T_e^{-0.45}\ \nu^{-0.1}\ S_\nu D^2 \qquad (1a)$$

Here D is the distance in kpc between the sun and the HII region, T_e in degree K is the electron temperature, y^+ the number abundance of ionized helium and $a(\nu,T_e)$ a factor of order unity. The Lyc photon production rate, N_{Lyc}, is related to N'_{Lyc} by

$$N'_{Lyc} = (1-f_{esc})f_{net}\ N_{Lyc} \qquad (1b)$$

with f_{esc} the fraction of Lyc photons which escape from the HII region and $(1-f_{net})$ the fraction of Lyc photons which are directly absorbed by dust. The total radio and IR spectrum of a typical radio HII region (i.e. a relatively young HII region with central emission measures of $\gtrsim 10^4$ pc cm^{-6} and angular diameters of some arc minutes or less) is shown in Fig. 1.

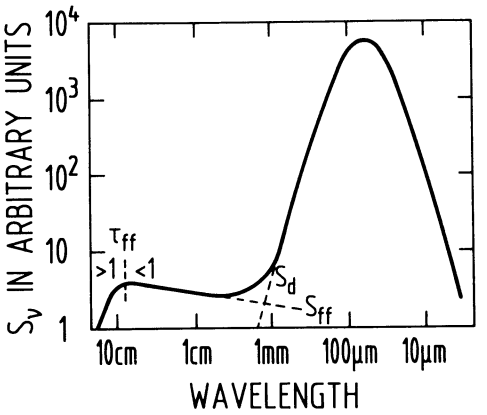

Fig. 1: Typical spectrum of a radio HII region. At higher frequencies (τ_{ff} <1) $S_{ff} \propto \nu^{-0.1}$. To a first approximation the spectrum of the dust emission can be approximated by a modified Planck function $S_d \propto \nu^m B_\nu(T_c)$.

The steep increase of the spectrum at wavelengths $\lesssim 1$ mm is due to thermal emission from dust grains. This part of the spectrum can usually be approximated by the modified Planck-function $\nu^m B_\nu(T_d)$, with m ~2 and T_d a mean temperature of the dust grains. The integrated spectrum yields the IR luminosity, L_{IR}, which is related to the total stellar luminosity of the ionizing star(s), L_*, by

$$L_{IR} = f_d L_*$$

with f_d the fraction of the stellar luminosity which is absorbed and reradiated by dust.

Finally, the ratio of the integrated line intensities of two adjacent radio recombination lines of H and He yields immediately the number abundance of ionized helium

$$y^+ = n(He^+)/n(H^+) \qquad (3)$$

https://doi.org/10.1017/S0074180900149435 Published online by Cambridge University Press

averaged over the HII region. Knowing the true He-abundance, y = n(He)/n(H), one can infer the ratio of He ionizing Lyc photons to the total number of Lyc photons of the ionizing star(s), (see, e.g. Mezger, 1979).

The derivation of star formation rates (SFR) from Lyc photon production rates.

This procedure is straight forward and has most recently been discussed by Güsten and Mezger (1983; hereafter referred to as Paper I). In a first step one separates thermal (free-free) and nonthermal (synchrotron) emission using radio continuum surveys made at two widely separated frequencies. This yields N'_{Lyc} (see eq. (1a)) and - with appropriate corrections - via eq. (1b) the total Lyc photon production rate N_{Lyc} of all O stars in the region under consideration.

The formation rate of O stars is linked to the total SFR by the Initial Mass Function (IMF). As usual we separate the creation function, i.e. the number of stars formed per unit time in the mass interval m, m+dm, into a time-dependent SFR $\Psi(t)$ (in units of $m_\odot$ yr^{-1}) and a time-independent initial mass function (IMF) $\phi(m)$, with upper and lower mass limits m_u and m_L, respectively. The IMF is normalized in the usual way, viz.

$$\int_{m_L}^{m_u} \phi(m)\,m\,dm = 1$$

In the following discussion we consider the IMF derived by Salpeter (1955; $\phi(m) \propto m^{-2.35}$) and by Miller and Scalo (1979; $\phi(m) \propto m^{-3.62}$ for $m \gtrsim 30\ m_\odot$) as limiting cases for O stars. With the assumption that the present-day SFR, $\Psi(t_o)$, did not change during the main sequence (MS) lifetime of O stars, τ_{MS}, we derive in Paper I the following relation between Lyc photon production rate $N_{Lyc}(t_o)$ and SFR $\Psi(t_o)$

$$N_{Lyc}(t_o) = \Psi(t_o) \int_{m_L}^{m_u} \phi(m)\,dm \int_0^{\tau_{MS}(m)} N_{Lyc}(m,\tau)\,d\tau \qquad (4)$$

The ratio of Lyc photon luminosity to SFR can be computed for a given IMF $\phi(m)$ from stellar model atmospheres. In Fig. 2 is shown the product $\phi(m)\ N_{Lyc}(m)$ for the two IMFs. If multiplied with $\tau_{MS}(m)$ the maximum of the corresponding curves is shifted towards stars with masses m = 30–40 $m_\odot$. This means that stars of spectral type O7–O6 are the main contributors to the Lyc photon production rate in the galactic plane. Contributions of stars with $m \lesssim 10\ m_\odot$ (i.e. sp. type B2 and later) are negligible. Hence we have to extend the integration only over $m \geq 10\ m_\odot$. Convenient numerical expressions for the quantity

https://doi.org/10.1017/S0074180900149435 Published online by Cambridge University Press

$$\frac{\langle N_{Lyc}(t,\phi)\rangle}{\Psi(t)} = \phi(1)\cdot P(\phi) = \left\{ \int_{m_L'}^{m_u} \phi(m)\,m\,dm \right\}^{-1} \int_{10m_\odot}^{m_u} \phi(m)\,dm \int_0^{\tau_{MS}(m)} N_{Lyc}(m,\tau)\,d\tau \qquad (5a)$$

are given in Paper I. Note that (5a) depends on the lower mass limit m_L' through the normalization factor of $\phi(m)$, which is

$$\int_{m_L'}^{m_u} \phi(m)\,m\,dm = \begin{cases} 1 & \text{for } m_L' = m_L \\ 1-\Delta(m_c) & \text{for } m_L' = m_c > m_L \end{cases} \qquad (5b)$$

$$\text{with } \Delta(m_c) = \int_{m_L}^{m_c} \phi(m)\,m\,dm \quad \text{and} \quad 1-\Delta(m_c) = 0.80\, m_c^{-0.4} - 0.23 \qquad (5c)$$

for the Miller-Scalo IMF, $m_L = 0.1\ m_\odot$ and $1 \leq m_c/m_\odot \leq 6$. All numerical values given in the following relate to this IMF.

The SFR which corresponds to a given Lyc photon production rate at a time t is

$$\Psi(t) = N_{Lyc}(t)/\phi(1)P(\phi) \qquad (5d)$$

of which the fraction $\frac{dM_*}{dt} = (1-r)\Psi$ is permanently locked up in stars. $\phi(1)P(\phi) = 2.5\ 10^{52}$ Lyc photons $s^{-1}/m_\odot\ yr^{-1}$ is the number of Lyc photons produced per sec per solar mass per year of gas converted into stars (Paper I), r = 0.42 is the "instantaneous return rate".

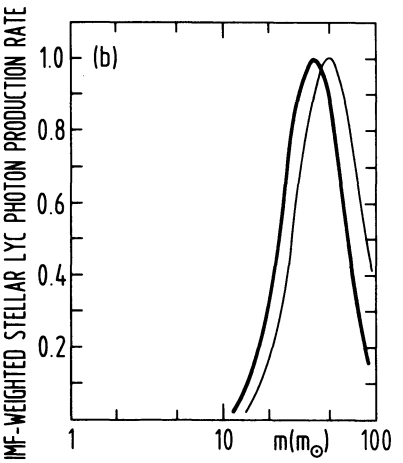

Fig. 2: The IMF weighted stellar Lyc photon production rate (Cox et al., 1985). The thin solid curve relates to the Salpeter IMF, the heavy solid curve relates to the Miller-Scalo IMF.

https://doi.org/10.1017/S0074180900149435 Published online by Cambridge University Press

Global present-day SFRs in the Galactic Disk derived for a constant IMF

In Paper I we estimate a Lyc photon production rate in the galactic disk of

$$\sum_{R=2}^{10} N_{Lyc}(R) = 2.6(^{+0.8}_{-0.5})\ 10^{53}\ s^{-1} \tag{6a}$$

Substitution in eq. (5d) yields a present-day SFR in the galactic disk of

$$\sum_{R=2}^{10} \Psi(t_o,R) \sim 10.4\ m_\odot\ yr^{-1} \tag{6b}$$

(The SFR in the central region R <2 kpc amounts to ∿10% of the above value; that outside R >10 kpc amounts to less than 10%).

This value has to be compared to the SFR $<\Psi(t)>$, averaged over the age of the galactic disk, τ_{Disk}. With a total stellar mass of the galactic disk of $\sum_{R=2}^{10} M_*(R) = 6.1\ 10^{10}\ m_\odot$, an "instantaneous return rate" r ∿0.42 of the gas transformed into stars and an estimated age of the galactic disk of $\tau_{Disk} \sim 10^{10}$ yr, this average value is

$$<\Psi> = \frac{1}{(1-r)} \frac{\Sigma M_*}{\tau_{Disk}} \sim 10.3\ m_\odot\ yr \tag{7a}$$

If star formation is a continuous process and if stars and interstellar matter in the galactic disk form a closed system (i.e. negligible infall of gas from the halo or radial gas flow), then a ratio $\Psi(t_o)/<\Psi> \gtrsim 1$ is difficult to reconcile with a power-law dependence of the SFR on the total mass of gas available to be transformed into stars. A relation of the type $\Psi \propto M_{gas}^k$ yields for a closed system ratios of present-day to average SFRs of

$$\frac{\Psi(t_o)}{<\Psi(t)>} = \begin{cases} 1 & \text{for } k = 0 \\ \frac{\mu \ell n \mu^{-1}}{1-\mu} = 0.134 & \text{for } k = 1 \end{cases} \tag{7b}$$

which means that for k = 1 (and quite generally for k >0) the ratio $\Psi(t)/<\Psi(t)>$ decreases with time, since $\mu = M_{gas}/M_{tot}$ decreases with time. The numerical value of ∿13% for k = 1 holds for μ ∿0.04, the present-day gas-to-total mass ratio averaged over the galactic disk (R = 2-10 kpc), as inferred from observations. A present-day SFR of

https://doi.org/10.1017/S0074180900149435 Published online by Cambridge University Press

$\sim$10 $m_\odot$ yr^{-1} would mean a time-independent SFR; it would also mean that the remaining ISM of the galactic disk would be locked up in stars within some 10^8 years.

If one accepts the much more likely situation of a SFR which continuously decreases with time one has to face the fact that for a present-day SFR $\Psi(t_o) < <\Psi(t)>$ there are too many Lyc photons produced. To reconcile the observed high Lyc photon production rate with a reasonably low SFR we suggest that the local IMF, determined from star counts in the solar vicinity, does not hold throughout the galactic disk. We further suggest that spatial bimodal star formation yields the appropriate modification of the IMF.

SFRs of O stars.

From observations we know that O stars form out of molecular clouds both in the spiral arms (sa) and in the interarm region (ia). The surface density of O stars in spiral arms is much higher than in the interarm region. While the O star SFR in the interarm region appears to be proportional to the amount of ISM contained in molecular clouds to some power k, $\Psi_{OB}^{ia} \propto M_{H_2}^k$, additional O star formation is induced if the ISM flows into spiral arms. We assume that there the O star SFR is proportional to the amount of ISM that flows per unit time through the spiral arms. This amount is determined by the orbital velocity of the ISM $R\Omega_R$, relative to the pattern speed, $R\Omega_P$, of the spiral arms. Integrated over a concentric annulus of radius R and width ΔR = 1 kpc the O star SFR is

$$\Psi_{OB}^{(R)} = \Psi_{OB}^{ia} + \Psi_{OB}^{sa} \propto M_{H_2}^k(R)[1+\alpha\nu(R)] \qquad (8a)$$

Here $\alpha = \Psi_{OB}^{sa}(R_\odot)/\Psi_{OB}^{ia}(R_\odot)$ is the ratio of O stars formed in spiral arms and in the interarm region, respectively, at the distance of the solar circle, $R_\odot$, while

$$\nu(R) = \frac{\Omega_R - \Omega_P}{\Omega_\odot - \Omega_P} \qquad (8b)$$

is the increase of induced star formation in spiral arms at distance R relative to that at $R = R_\odot$. For a derivation of these relations and convenient numerical approximations see Paper I. $\nu(R)$ is given in column (8) of Table 1.

With $N_{Lyc} \propto \Psi_{OB}$ we can check the validity of the adopted law of the formation rate of massive stars. In Fig. 3 are plotted as a histogram the "observed" Lyc photon production rates $N_{Lyc}(R)$ from Table 1, column (5). Substitution of M_{H_2} (column (2c)) in eq. (8a) and normalization to $\sum_{1}^{10}$[const $M_{H_2}^k(1+\alpha\nu)$] = 2.52 10^{53} s^{-1} yields the points plotted for k = 1, 1.5 and 2, respectively. We see that eq. (8a) with $1 \leq k \leq 1.5$ fits the observed Lyc photon production rate reasonably well. In the following we adopt, for convenience, k = 1. Observations suggest that at $R_\odot$ = 10 kpc equal amounts of O stars are formed in spiral arms and in the interarm region, i.e. α = 1. Integrated over the galactic disk (R = 2-10 kpc)

https://doi.org/10.1017/S0074180900149435 Published online by Cambridge University Press

this means $\Psi^{sa}/(\Psi^{ia}+\Psi^{sa}) \sim 0.7$, i.e. 70% of all O stars are formed in spiral arms.

Table 1: Star Formation Rates $\Psi(t_o)$ and Rates at which Matter is permanently locked up in Low Mass Stars and Stellar Remnants, (dM_*/dt), for Constant (Columns (6) and (7)) and Bimodal (Columns (9) and (10)) Star Formation and Related Quantities.

R (kpc)	M_{ISM}	M_{HI}	M_{H_2}	M_*	$\mu=$	N_{Lyc}	$\Psi(t_o)$	dM_*/dt	$\nu(R)$	$\Psi^{bm}(t_o)$	$(dM_*/dt)^{bm}$	$(dM_*/dt)^{pred}$	
	$(10^8\ m_\odot)$			$(10^9\ m_\odot)$	M_{ISM}/M_*	$(10^{52}\ s^{-1})$	$(m_\odot\ yr^{-1})$			$(m_\odot\ yr^{-1})$		$(m_\odot\ yr^{-1})$	
												k = 0	k = 1
	(2a)	(2b)	(2c)	(3)	(4)	(5)	(6)	(7)	(8)	(9)	(10)	(11)	(12)
2 - 3	0.6	0.24	0.36	5.6	0.011	1.01	0.40	0.23	5.41	0.17	0.05	0.53	0.03
3 - 4	1.0	0.34	0.66	7.3	0.014	1.84	0.74	0.43	4.05	0.31	0.11	0.73	0.04
4 - 5	2.3	0.74	1.56	8.6	0.027	5.47	2.18	1.26	3.17	0.99	0.37	0.86	0.09
5 - 6	3.5	0.84	2.66	9.6	0.036	6.81	2.72	1.58	2.57	1.33	0.52	0.96	0.12
6 - 7	3.3	0.76	2.54	8.8	0.038	3.60	1.44	0.84	2.10	0.75	0.31	0.88	0.11
7 - 8	3.9	1.95	1.95	8.2	0.048	3.53	1.41	0.82	1.74	0.77	0.33	0.82	0.13
8 - 9	3.3	1.95	1.35	6.7	0.049	2.61	1.04	0.60	1.43	0.60	0.27	0.67	0.10
9 - 10	3.4	2.28	1.12	6.4	0.053	1.31	0.52	0.30	1.14	0.32	0.15	0.64	0.11
Σ(R=2-10)	21.3	9.10	12.20	60.9		26.2	10.4	6.1		5.24	2.11	6.1	0.73

*) M_{ISM}, M_{HI} and M_{H_2} relate to the total mass of interstellar matter, i.e. the contribution of heavy elements is included.

https://doi.org/10.1017/S0074180900149435 Published online by Cambridge University Press

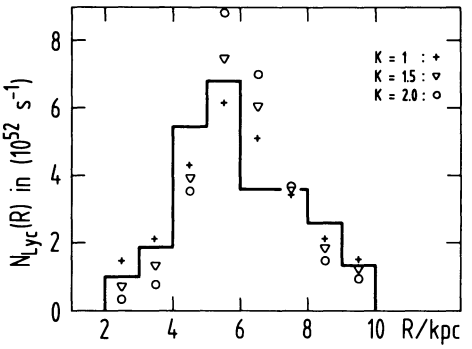

Fig. 3: The Lyc photon production rate in the galactic disk as derived from radio free-free emission (histogram) is compared to an O star formation rate of the form $\Psi_{OB}(R) \propto M_H^K (1+\alpha\nu)$. *(See text).*

Spatial bimodal star formation.

Spatial bimodal star formation means that in the interarm region stars form according to the IMF derived for the solar vicinity, i.e. in the total mass range m_L, m_u while only stars above a critical mass $m \geq m_c$ form by induced star formation such as in spiral arms. This was first suggested by Mezger and Smith 1977) based on a review of relevant observations. It was put into a quantitative form by Güsten and Mezger (1983; Paper I) to explain the existence of abundance gradients in the galactic disk as a consequence of chemical evolution. In the following we adopt $m_c = 3\ m_\odot$. It appears that in small molecular clouds in the interarm region low mass stars $\gtrsim 0.1\ m_\odot$ form first and OB stars form last, while in spiral arms (or - more generally - wherever star formation is induced by large-scale compression of molecular clouds) the massive stars form at about the same time and suppress the formation of low mass stars. Physicsl explanations for this process are summarized by Silk (this symposium).

With ϕ the IMF derived for the solar vicinity the bimodal IMF assumes the form

$$\phi^{bm}(R,\alpha,m_c) = N^{-1}\ [\phi^{ia} + \alpha\nu(R)\phi^{sa}] \qquad (9a)$$

with $\phi^{ia} = \phi(m \geq m_L)$, $\phi^{sa} = \phi(m \geq m_c)$. The normalization factor is

$$N = \int_{m_L}^{m_u} \phi^{bm}(R,\alpha,m_c)\,m\,dm = 1+\alpha\nu(R)[1-\Delta(m_c)] \qquad (9b)$$

$1-\Delta(m_c)$, as given by eq. (5c), yields 0.29 for $m_c = 3\ m_\odot$. The fraction of matter permanently locked up in stars is

$$(1-r)^{bm} = \frac{1}{1+\alpha\nu(R)[1-\Delta(m_c)]} \left\{ (1-r)^{ia} + \alpha\nu(R)(1-r)^{sa} \right\} \qquad (10a)$$

https://doi.org/10.1017/S0074180900149435 Published online by Cambridge University Press

with

$$(1-r)^{sa} = [0.6 \int_{m_c}^{6} \phi(m)dm + 1.4 \int_{6}^{m_u} \phi(m)dm] = 0.136\, m_c^{-1.4} + 0.008 \qquad (10b)$$

for $1 \leq m_c/m_\odot \leq 6$.

In the derivation of eqs. (10) it is assumed that the MS lifetime $\tau_{MS}(m \leq 1\ m_\odot) \gtrsim \tau_{Disk}$, that stars with $1 \leq m/m_\odot \leq 6$ evolve to white dwarfs with an average mass of $\sim 0.6\ m_\odot$, and more massive stars evolve to neutron stars with an average mass $\sim 1.4\ m_\odot$. For $m_c = 3\ m_\odot$, $m_u = 60\ m_\odot$ the fraction of gas transformed into stars which is permanently locked up in low mass and dead stars is $(1-r)^{ia} = 0.58$ in the interarm region and $(1-r)^{sa} = 0.04$ in spiral arms.

SFRs for spatial bimodal star formation

Substitution of ϕ^{bm} (eqs. 9a,b) in eq. (4) yields the Lyc photon production rate per solar mass of gas transformed per year into stars in the case of spatial bimodal star formation

$$\frac{\langle N_{Lyc} \rangle}{\psi^{bm}} = \phi(1)P^{bm}(\phi) = \phi(1)P(\phi)\, \frac{1+\alpha\nu(R)}{1+\alpha\nu(R)[1-\Delta(m_c)]} \qquad (11)$$

In the derivation of eq. (11) use has been made of eqs. (5a,b). $\phi(1)P(\phi) = 2.5\ 10^{52}\ s^{-1}/m_\odot\ yr^{-1}$ applies for the interarm region, $\phi(1)P(\phi)/[1-\Delta(m_c)]$ applies for spiral arms.

For a given Lyc photon production rate $N_{Lyc}(R)$ the corresponding SFR is

$$\psi^{bm}(R) = \frac{N_{Lyc}(R)}{\phi(1)P(\phi)} \left\{ \frac{1}{1+\alpha\nu(R)} + \frac{\alpha\nu(R)[1-\Delta(m_c)]}{1+\alpha\nu(R)} \right\} \qquad (12a)$$

and the fraction permanently locked up in low mass and dead stars is

$$\frac{dM_*^{bm}}{dt} = \psi^{bm}(1-r)^{bm} = \frac{N_{Lyc}(R)}{\phi(1)P(\phi)} \left\{ \frac{(1-r)^{ia}}{1+\alpha\nu(R)} + \frac{\alpha\nu(R)(1-r)^{sa}}{1+\alpha\nu(R)} \right\} \qquad (12b)$$

The first and second term in eqs. (12) relate to star formation in interarm and spiral arm region, respectively.

Dividing the Lyc photon production rates $N_{Lyc}(R)$ given in column (5) of Table 1 by $\phi(1)P(\phi) = 2.5\ 10^{52}\ s^{-1}/(m_\odot\ yr^{-1})$ yields the SFR $\Psi(t_o,R)$ for constant IMF listed in column (6), and the lock-up rates of matter, $dM_*(R)/dt = 0.58\Psi(R)$, listed in column (7). The corresponding values for spatial bimodal star formation are given in column (9) and (10).

https://doi.org/10.1017/S0074180900149435 Published online by Cambridge University Press

Nearly all the matter that is permanently locked up in low mass and dead stars (viz. 1.82 $m_\odot$ yr^{-1}) comes from star formation in the interarm region. This is the reason why $(dM_*(R)/dt)^{bm}$, shown in Fig. 4 by open triangles, is much flatter than the corresponding rate obtained for a constant IMF (shown by open circles), where the induced SFR in spiral arms leads to an enormous lock-up rate in low mass and dead stars in the range between R = 4 and 8 kpc. For comparison purposes are also shown in Fig. 4 the predicted lock-up rates assuming a closed system and a power-law dependence of SFR on the mass of interstellar matter.

$$(dM_*/dt)^{pred} = \frac{M_*(R)}{\tau_{Disk}} \begin{cases} 1 \text{ for } k = 0 \\ \dfrac{\mu \ell n \mu^{-1}}{1-\mu} \text{ for } k = 1 \end{cases}$$

Here we substituted for $\tau_{Disk} = 10^{10}$ yr and for M_* and μ the values given in columns (3) and (4) of Table 1. While the lock-up rates averaged over the galactic disk, $\sum_{R=2}^{10}(dM_*/dt)$, derived for constant IMF and predicted for constant SFR (k=0) (lowest line of columns (7) and (11)) agree well their radial variations, as shown in Fig. 4, are incompatible. The present lock-up rate predicted for k=1, 0.73 $m_\odot$ yr^{-1}, (column (12)), is by about a factor of three lower than the value derived for the specific model of spatial bimodal star formation to which the values in column (10) relate. Remember that we use here a model developed in Paper I to explain abundance gradients. The above discrepancy is partly resolved if we use a more realistic model with a gradual build-up of the galactic disk by infalling halo gas. For an exponentially decreasing accretion rate ($\propto \exp\{-t/\tau\}$, $\tau \sim 5$ Gyr) Vader and de Jong (1981) have shown that even for k = 1 values $\langle\Psi\rangle/\Psi(t_o) > 1$ are possible.

Much more important than the total SFR integrated over the galactic disk is the rate at which matter is permanently locked up in low mass stars and stellar remnants and especially its radial dependance which - integrated over the age of the disk - determines the present-day mass distribution of the disk. Bimodal star formation leads to a radial dependence of the present-day lock-up rate $(dM_*/dt)^{bm}$ which agrees in shape reasonably well with that predicted from the present-day mass distribution M*(R). To demonstrate this agreement we have arbitrarily multiplied $(dM_*/dt)^{pred}_{k=1}$ by a factor of three (dotted line in Fig. 4). A justification for such an increase is given above by gradual accretion of the disk.

Note that eqs. (7b and 13) hold for a closed system with $\mu = M_{ISM}/M_{tot}$ and M_{ISM} the total mass of interstellar matter, while eq. (8a) relates the SFR to the mass of hydrogen in molecular form. Formally this can be justified if eq. (8a) is rewritten as a relation for the lock-up rate

$$(dM_*/dt)^{bm} \sim (dM_*/dt)^{ia} \propto M_{ISM}^{k} \qquad (13)$$

https://doi.org/10.1017/S0074180900149435 Published online by Cambridge University Press

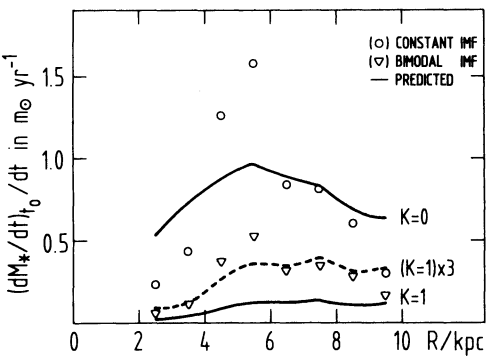

Fig. 4: The rate at which ISM is locked up in low mass and dead stars. Solid and dotted curves: Predicted from the observed mass distribution in the galactic disk and an adopted relation $(dM_*/dt) \propto M_{ISM}^k$ with k = 0, 1. Dots and triangles: Lock-up rates derived from observed Lyc photon production rates and with a constant and bimodal IMF, respectively.

since matter is permanently locked up in low-mass stars predominantly in the interarm region. This allows us to use solutions for the closed system with $M_{ISM} + M_* = M_{tot}$ to compute the "predicted" lock-up rates given in columns (11) and (12) of Table 1 for k = 0 and 1, respectively, and shown in Fig. 4. In the case of spatial bimodal star formation the star formation in spiral arms appears like a (compared to the galactic rotation time) short firework, which leaves most of the ISM transformed into stars as ashes in the form of ISM enriched with heavy elements, while only a small fraction (viz. ∿4%) remains permanently locked up in stellar remnants. In the interarm regions, on the other hand, about equal amounts of the ISM transformed into stars are returned "instantaneously" to interstellar space and permanently locked up predominantly in low mass stars. Hence it is star formation in the interarm region that accounts for the present-day stellar mass distribution in the galactic disk.

Other applications of bimodal star formation

It should be stressed that spatial bimodal star formation was initially introduced to explain the existence of element abundance gradients in the galactic disk. The different return rates in spiral arms and interarm regions, respectively, of gas processed in intermediate and massive stars, together with the increasing fraction of intermediate and massive stars, formed in spiral arms with decreasing galactocentric distance R, accounts for the variable yield required for an explanation of the observed abundance gradients. (Paper I and Güsten, 1985).

With a generalized concept of bimodal star formation, i.e. whenever star formation is induced by some large-scale effects such as in starbursts (observed in the central regions of some galaxies and in galaxies with extreme infrared emission), the derived extremely low mass-to-luminosity ratios can be explained (Silk, this symposium).

The secondary maximum, which appears in IMFs derived from observed luminosity functions with SFRs decreasing with time, find a natural explanation by spatial bimodal star formation (see Scalo, this symposium).

Larson (1985) has constructed a star formation model that is bimodal in time, which can account for all of the unseen mass in the solar neighbourhood in the form of stellar remnants, as well as for many other observed characteristics of spiral galaxies.

https://doi.org/10.1017/S0074180900149435 Published online by Cambridge University Press

Luminous MS stars and infrared emission from warm dust

Dusty galaxies emit a large fraction of their stellar luminosity as thermal infrared emission from dust. The IR spectrum of the inner part of our Galaxy (R $\lesssim$8 kpc), as taken from Cox, Krügel and Mezger (1985; hereafter referred to as Paper II) is shown in Fig. 5. The spectrum can be decomposed into contributions of cold (10-25 K) dust, warm (30-40 K) dust and hot (250-500 K) dust. The total IR luminosity is $\sim$1.5 10^{10} $L_\odot$ or $\sim$30% of the total stellar luminosity; the luminosity of warm and hot dust are $\sim$5.7 10^9 $L_\odot$ and $\sim$1.7 10^9 $L_\odot$, respectively.

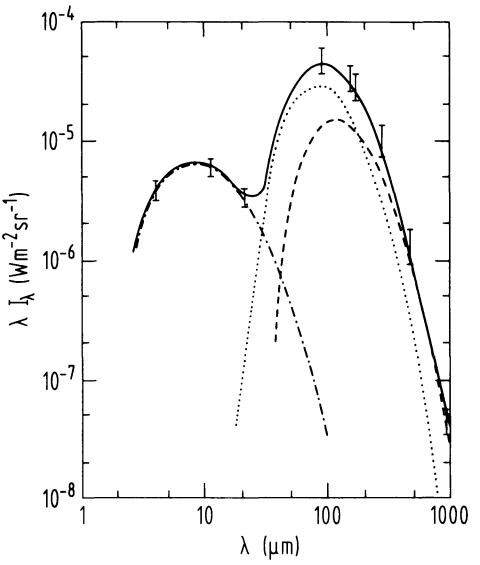

Fig. 5: Spectrum of the dust emission from the inner part (R $\lesssim$8 kpc) of our Galaxy averaged over galactic longitudes 3-35° and latitudes $|b|$ >1°. Our analysis in Paper II shows that the spectrum can be decomposed in contributions from: i) cold (10-25 K) dust associated with atomic and molecular hydrogen heated by the general ISRF (dashed curve); ii) warm (30-40 K) dust heated by OB stars (dotted curve); and iii) hot (250-500 K) dust heated by M giants with heavy mass loss.

For each of these three dust components a dominant heating source has been identified (Paper II and references therein): Cold dust is heated by the general interstellar radiation field, warm dust is heated by O and B stars, hot dust is heated by OH/IR stars, i.e. M giants with heavy mass loss. Hence, it is only warm dust which traces luminous MS stars. As can be seen from Fig. 5 the spatial distribution of warm dust emission should be well represented by emission at $\lambda \sim 60$ μm, where IRAS data will soon become available.

With eq. (2) one can formally write a relation between warm dust luminosity and SFR which is analoguous to eq. (4):

$$L_{IR}^{wd}(t_o) = \Psi(t_o) \int_{m_L}^{m_u} \phi(m) f_d(m) dm \int_0^{\tau_{MS}(t)} L_*(m,\tau) d\tau \qquad (14)$$

In Fig. 6 is shown the product $\phi(m)L_*(m)$. The two curves behave qualitatively like the curves $\phi(m)N_{Lyc}(m)$ shown in Fig. 2, but peak at lower stellar masses, viz. $\sim$13 $m_\odot$ (spectr. type BI) and $\sim$28 $m_\odot$ (O7), respectively. However, when multiplied with the main sequence lifetime $\tau_{MS}(m)$, the stellar luminosity curves diverge, while the maxima of the Lyc photon luminosity curves are only shifted toward lower stellar masses.

https://doi.org/10.1017/S0074180900149435 Published online by Cambridge University Press

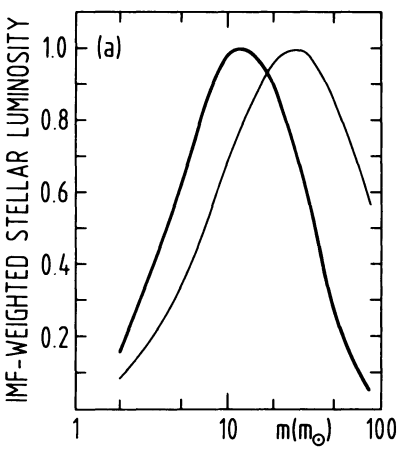

Fig. 6: The IMF weighted stellar luminosity. The thin solid curve relates to the Salpeter IMF, the heavy solid curve relates to the Miller-Scalo IMF. (Cox et al., 1985).

This means that the factor $f_d(m)$, i.e. the fraction of stars of a given stellar mass which contribute to the heating of warm dust, governs the computed ratio of warm dust luminosity of the SFR. Since this fraction is very difficult to estimate for stars later than OB, SFRs derived from IR luminosities are rather unreliable.

For our galaxy we know for $R \leq 10$ kpc both the total Lyc photon luminosities, $N_{Lyc} = 2.6\ 10^{53}\ s^{-1}$ and the warm dust luminosity, $L_{IR}^{wd} = 7.3\ 10^9\ L_\odot$ (Paper II), so that

$$\frac{<N_{Lyc}>}{<L_{IR}^{wd}>} = 3.56\ 10^{43}\ s^{-1}\ L_\odot^{-1} \qquad (15a)$$

On the assumption that this ratio is typical for galaxies with a high formation rate of luminous stars one can derive an empirical factor for converting observed warm dust IR luminosities into SFRs, which is

$$\Psi(t) = \frac{3.5\ 10^{43}\ L_{IR}^{wd}}{\phi(1)P(\phi)}\ [1-\Delta(m_c)] = 1.4\ L_{IR,9}^{wd}\ [1-\Delta(m_c)] \qquad (15b)$$

Here $\Psi(t)$ is in $m_\odot\ yr^{-1}$, $L_{IR,9}$ in $10^9\ L_\odot$ and $\Delta(m_c)$ is given by eq. (5c). As an example consider a star-burst galaxy with $L_{IR} \sim 10^{11}\ L_\odot$. If stars of all masses were produced in the star burst a SFR of 140 $m_\odot\ yr^{-1}$ would be required to sustain this luminosity, of which 81 $m_\odot\ yr^{-1}$ would be permanently locked up in low mass stars and stellar remnants. If only stars above $m_c \sim 3\ m_\odot$ were formed the corresponding rates are $\Psi = 39\ m_\odot\ yr^{-1}$ and $dM^*/dt = 5.6\ m_\odot\ yr^{-1}$.

Luminous post MS stars and infrared emission from hot dust

The dust emission spectra of our Galaxy (Fig. 5) and of external galaxies show a secondary maximum around $\lambda \sim 10$ μm. It corresponds to hot dust in the temperature range 250-500 K. The hot dust luminosity in our Galaxy is $L_{IR}^{hd} \sim 1.7\ 10^9\ L_\odot$ or ∼10% of the total IR luminosity. There are two competing explanations for this "M(=middle) IR shoulder".
i) The existence of very small grains, made of polycyclic aromatic molecules, which have spectral features between $\lambda = 3.7$ and 11.9 μm.

https://doi.org/10.1017/S0074180900149435 Published online by Cambridge University Press

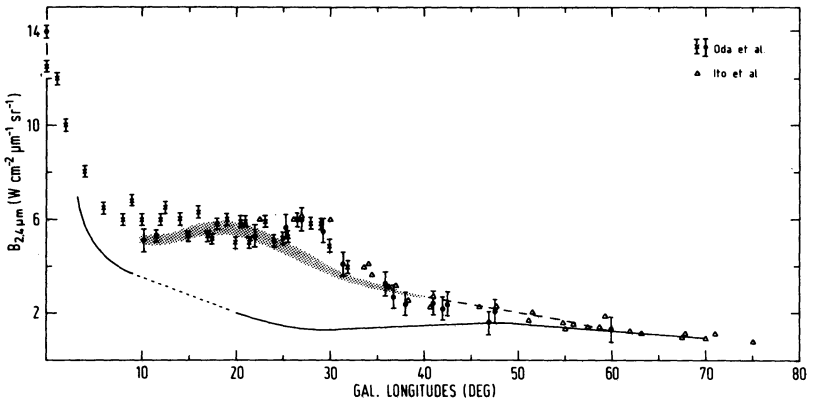

Fig. 7: The ridge line intensity at λ2.4 μm as observed by Oda et al. (1979) and Ito et al. (1977). The solid curve relates to model computations, where the space density of M giants in the solar vicinity is scaled with the total mass distribution and dust opacity at λ2.4 μm is considered. The shaded curve relates to a model, where an excess component of medium mass M giants is superimposed on the distribution of old disk population M giants. The radial distribution of this excess component is similar to that of the present-day O stars. This excess component finds a natural explanation if i) spatial bimodal star formation applies, ii) all stars in the mass range $m_c \sim 3\ m_\odot \leq m \lesssim 8\ m_\odot$ evolve to M giants, and iii) the SFR in the galactic disk was approximately constant over the past 10^8 yr (Güsten and Mezger, 1983; Paper I).

When heated by absorption of an energetic photon to temperatures of ∿600 K these grains emit predominantly in the MIR range and thus may account for the MIR shoulder (Léger and Puget, 1984);
ii) the presence of some 10^4 M giants in the galactic plane with heavy mass loss ($\dot{M} \gtrsim 10^{-5}\ m_\odot\ yr^{-1}$) and typical luminosities of some $10^4\ L_\odot$ which emit all their radiation in the MIR. (Paper II).

In Paper II we conclude that both explanations apply and that the observed MIR shoulder in our and external galaxies is due to a superposition of the two mechanisms. The small particles explain observations of the MIR shoulder in dust heated by the general ISRF, e.g. in the IRAS "cirrus clouds" at high galactic lattitudes. The M giants with mass loss and MIR emission from surrounding dust shells, observationally known as OH/IR stars, explain the strong MIR emission close to the galactic plane.

Owing to 2.4 μm surveys of the galactic plane especially by Japanese groups (see, e.g. Hayakawa et al., 1977) it is well known that there exists a large number of M giants, which account for a total luminosity of $\sim 2.10^{10}\ L_\odot$ (see, e.g. Mathis et al., 1983). The ridge line intensity of the 2.4 μm emission is shown in Fig. 7. It consists of contributions from old disk population M giants (shown in Fig. 7 as (interrupted) solid curve) and an excess component of M giants which accounts for a

https://doi.org/10.1017/S0074180900149435 Published online by Cambridge University Press

total luminosity of $\sim 6\ 10^9\ L_\odot$. In Paper II it is shown that this excess component can be explained if all stars with $m > m_c \sim 2\text{-}3\ m_\odot$ evolve to M giants and if their distribution in the galactic plane is similar to that of O stars. Remember that m_c is the critical lower mass in spatial bimodal star formation.

The inference of the NIR ($\lambda 2.4\ \mu m$) emission is that its "excess component" relates to post MS stars in the mass range $m \sim 3\text{-}8\ m_\odot$, which have evolved to M giants. The inference of the MIR ($\lambda \sim 10\ \mu m$) emission is that it relates to a subgroup of these medium mass M giants viz. those, which are in a (necessarily relatively short-living) phase of heavy mass loss. Now remember that the MS lifetime of a $3\ m_\odot$ star is $\sim 3\ 10^8$ yr. With a reasonable estimate of luminosity integrated over post MS lifetimes of intermediate mass stars we arrive at the conclusion that the present-day SFR is compatible with the number of intermediate mass M giants observed today through their NIR emission. On this basis we suggest that the SFR of luminous stars in the galactic disk was rather constant at least during the last galactic rotation (Paper I).

Ionization state of HII regions and the upper mass limit of the IMF

While the ^4He abundance in the galactic disk appears to increase towards the galactic center the ionized helium abundance observed in giant HII regions actually starts to decrease at galactic radii R $\sim$8-9 kpc. (For the latest review of radio recombination line observations see Mezger and Wink, 1983).

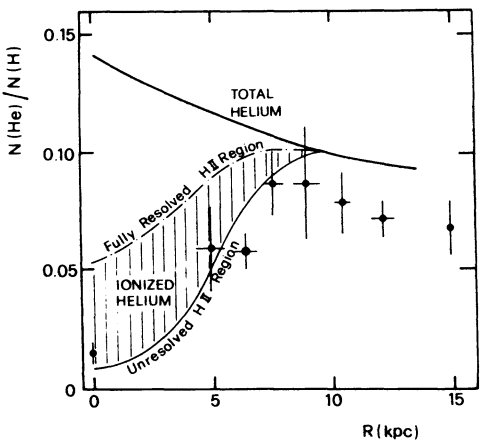

Fig. 8: Observed He^+ abundances (-•-) are compared to model computations. Heavy solid curve: Adopted He abundance. Thin solid curves: Results of model computations where $<T_{eff}>$ decreases with R (Panagia, 1979).

This means that with decreasing galactocentric distance the He^+ Strömgren sphere shrinks relative to that of ionized hydrogen. Panagia (1979) interprets this effect as a decrease of the average effective temperature, which characterizes the Lyc radiation field in giant HII regions, according to

$$<T_{eff}> = 3.1\ 10^4 \exp\{R_{kpc}/50\} \quad \text{in K} \qquad (16)$$

Panagia links this decreases of $<T_{eff}>$ to the increase of the metal abundance Z with decreasing R. Blanketing of UV lines with an increase of the stellar radius on the one hand, and a decrease of the upper IMF

https://doi.org/10.1017/S0074180900149435 Published online by Cambridge University Press

mass limit on the other hand should contribute about equally to this effect. Such a decrease of $m_u \propto Z^{-0.5}$ was in fact predicted by Kahn (1974) based on an accretion theory for the formation of massive stars.

REFERENCES

Cox, P., Krügel, E., Mezger, P.G. (1985) Astron. Astrophys. (in print) (Paper II)
Güsten, R. (1985) "The Chemical Evolution of the Milky Way", Erice Lectures, preprint
Güsten, R., Mezger, P.G. (1983) Vistas in Astronomy 26, 159 (Paper I)
Hayakawa, S., Ito, K., Matsumoto, T., Ugama, K. (1977) Astron. Astrophys. 58, 325
Ito, K., Matsumoto, T., Uyama, K. (1977) Nature 256, 517
Kahn, F.D. (1974) Astron. Astrophys. 37, 149
Larson, R.B. (1985) "Bimodal star formation and remnant-dominant galactic models", preprint, subm. to MNRAS
Léger, A., Puget, J.L. (1984) Astron. Astrophys. 137, L5
Mathis, J., Mezger, P.G., Panagia, N. (1983) Astron. Astrophys. 128, 212
Mezger, P.G. (1979) in "Radio Recombination Lines", (P.A. Shaver, ed.), D. Reidel Publ. Co., p. 81
Mezger, P.G., Wink, J. (1983) Proc. ESO Workshop on "Primodial Helium", (Shaver, Kunth, and Kjär, eds.), p. 281
Miller, G.E., Scalo, J.M. (1979) Astrophys. J. Suppl. 41, 513
Oda, N., Maihara, T., Sugiyama, T., Okuda, H. (1979) Astron. Astrophys. 72, 309
Panagia, N. (1979) in "Radio Recombination Lines", (P.A. Shaver, ed.), D. Reidel Publ. Co., p. 99
Salpeter, E.E. (1955) Astropyhs. J. 121, 161
Vader, J.P., de Jong, T. (1981) Astron. Astrophys. 100, 124

Discussion : MEZGER.

ZINNECKER :

The Lyman continuum production rate does not depend on the upper mass limit using the Miller and Scalo IMF but peaks for $M \sim 30 M_{\odot}$ you said. How is it possible then to get a handle on the upper mass limit as a function of metallicity?

MEZGER :

What counts for the He ionization structure is not the Lyc photon production rate but rather the ratio of the ionizing photons to all Lyc photons, a quantity which depends strongly on $\langle T_{eff} \rangle$ and hence on the upper mass limit M_u.

SILK :

I do not think you are on very secure ground in appealing to the theoretical prediction that the upper mass limit depends on metallicities in a specific way in order to account for the radial gradient in the hardness of the ionizing photon flux. For example, the theoretical calculations assume spherical symmetry, yet the situation studied in which radiation from the accreting core interacts with an infalling shell is Rayleigh-Taylor unstable. I suspect that this can only allow additional accretion : in any case, additional simulations are needed. Is there any other viable mechanism for giving a gradient in selective absorption of Lyman continuum photons as the metallicity changes, for example due to line blankting or to small grain properties in HII regions?

MEZGER :

Maybe Kahn's theory oversimplifies the actual situation. But model fitting to the observed IR/submm spectra of compact HII regions shows that the inner region is heavily depleted in dust but that dust cocoons form at distances of .. 10^{17} cm from the surface of O stars, probably as a result of radiation pressure; hence, radiation pressure may, in fact, limit the mass of the most massive stars and this effect should certainly depend on the dust-to-gas ratio and thus on the metal abundance.

https://doi.org/10.1017/S0074180900149435 Published online by Cambridge University Press